Environmental Science & Technology

pubs.acs.org/est

Article

Influence of Particle Size and Fragmentation on Large-Scale Microplastic Transport in the Mediterranean Sea

Victor Onink,* Mikael L. A. Kaandorp, Erik van Sebille, and Charlotte Laufkötter

Cite This: *Environ. Sci. Technol.* 2022, 56, 15528−15540

Read Online

ACCESS | Metrics & More | Article Recommendations | Supporting Information

ABSTRACT: Microplastic particles move three-dimensionally through the ocean, but modeling studies often do not consider size-dependent vertical transport processes. In addition, microplastic fragmentation in ocean environments remains poorly understood, despite fragments making up the majority of microplastic pollution in terms of the number of particles and despite its potential role in mass removal. Here, we first investigate the role of particle size and density on the large-scale transport of microplastics in the Mediterranean Sea and next analyze how fragmentation may affect transport and mass loss of plastics. For progressively smaller particle sizes, microplastics are shown to be less likely to be beached and more likely to reach open water. Smaller particles also generally get mixed deeper, resulting in lower near-surface concentrations of small particles despite their higher total abundance. Microplastic fragmentation is shown to be dominated by beach-based fragmentation, with ocean-based fragmentation processes likely having negligible influence. However, fragmentation remains a slow process acting on decadal time scales and as such likely does not have a major influence on the large-scale distribution of microplastics and mass loss over periods less than 3 years.

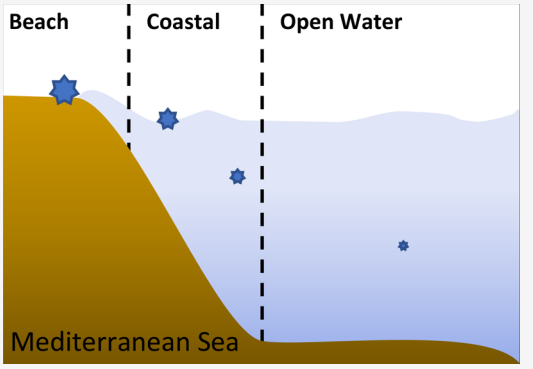

KEYWORDS: *Plastic pollution, Lagrangian modeling, Physical oceanography, Plastic fragmentation, Ocean plastic, Mediterranean Sea*

1. INTRODUCTION

Marine plastic pollution has negative ecological and economic impacts, such as harming marine wildlife through ingestion and entanglement[54,57,78] and reducing tourism at commercial beaches.[3,5] Plastic is ubiquitous in marine habitats, with microplastic (<5 mm) particles being found everywhere from coastlines to the deep sea.[9,10] Yet, the pathways and ultimate fate of plastic once it enters the ocean are not fully understood, complicating a full assessment of the associated risk of marine plastic pollution. A complete understanding of the fate of plastic once it enters the ocean is therefore necessary and urgent.

Lagrangian models are commonly used to explore various (micro)plastic scenarios and interpolate between the available measurements.[37,51,52,62,64,80] However, many models assume that all plastic is buoyant and remains at the ocean surface throughout the entire simulation. Furthermore, microplastic particles come in a wide array of sizes and densities, but models often assume one generic particle.[11,16,36,51,52,62,64,80] While these assumptions reduce model complexity, such models ignore all vertical transport processes and cannot be used to examine subsurface microplastic distributions. However, positively buoyant microplastic particles can be mixed below the ocean surface by wave-driven turbulence,[43,45,63] and buoyant polymers have been found on the seabed thousands of meters below the ocean surface.[6,9,82] Field measurements also indicate that the debris size affects the likelihood of the object reaching the open ocean, with smaller particles being more likely to escape coastal regions.[58] On a global scale, Mountford and Morales Maqueda[59] showed that the particle buoyancy can influence the large-scale transport both horizontally and vertically but did not explicitly relate these different buoyancies to particle sizes, while also using spatially coarse flow fields. Similarly, Huck et al.[36] demonstrated that over 80% of neutrally buoyant particles get mixed below 30 m but did not explicitly consider particle size and density, nor did they consider vertical turbulent mixing processes. In addition, plastic transport is further complicated by the various transformations that plastic particles undergo, such as changes in particle density due to biofouling,[28,29] decreasing particle size due to fragmentation,[30,75] and the influence of particle shape anisotropy on the particle behavior.[13,22] The fragmentation of microplastics into gradually smaller particles is suggested as a possible mass sink,[49] and it is important to understand the rate at which this

Received: May 11, 2022
Revised: August 11, 2022
Accepted: August 16, 2022
Published: October 21, 2022

could occur. Furthermore, while it is assumed that fragmentation generally occurs more quickly on beaches than in the open ocean due to higher UV exposure, higher oxygen levels, and greater temperature fluctuations,[2,37] there is limited experimental work that validates this assumption.

Understanding the influence that particle size has on large-scale transport is critical, as it can affect the particle buoyancy and therefore susceptibility to vertical mixing, as well as the bioavailability of the particles to marine organisms.[83] Here, we first present a series of Lagrangian experiments to investigate the influence of microplastic particle size and density on the large-scale transport. We limit our scope to the Mediterranean Sea, due to the availability of both field measurements[15,18,56,71] and modeling studies[38,39,76] to compare our results with. We then include microplastic fragmentation into our size-dependent transport framework, building upon the work from Kaandorp et al.,[39] to investigate the relative influence of ocean-based fragmentation. We also estimate the rate of mass transfer to plastic particles smaller than 0.156 mm (below the commonly used mesh size in microplastic observations, which is 0.33 mm).

2. METHODS

2.1. Ocean Reanalysis Data. For the 2010−2013 zonal and meridional currents, temperature, salinity, and Mixed Layer Depth (MLD) data, we use the CMEMS Mediterranean Sea Physics Reanalysis Product (CMSPRP),[27] which has a temporal resolution of 3 h, a horizontal spatial resolution of 1/24°, and 141 vertical depth levels. The model code is based on the NEMO version 3.6[53] ocean general circulation model (OGCM), and the reanalysis is forced with atmospheric forcing fields from the ECMWF ERA5 reanalysis.[33] The simulated Mediterranean circulation and salinity/temperature fields match well with observations.[26,35]

Since the CMSPRP does not account for wave forcing, we use the Mediterranean Sea Waves Reanalysis (MSWR)[44] for the peak wave period and meridional and zonal surface Stokes drift. This reanalysis product has a temporal resolution of 1 h and a horizontal spatial resolution of 1/24°. The model code is based on the ECMWF WAM 4.6.2 wave model[23] and is similarly forced with the ECMWF ERA5 reanalysis.[33]

For calculating the wind-driven turbulent mixing within the surface mixed layer, we use hourly 10 m surface wind fields from the ECMWF ERA5 atmospheric reanalysis[33] for consistency with the CMSPRP and MSWR products.

2.2. Lagrangian Transport. We use Parcels[21,47] to model plastic as virtual particles that are advected by the surface ocean currents. A change in the horizontal particle position $\vec{x}$ = (lon, lat) is calculated according to

$$\vec{x}(t + \Delta t) = \vec{x}(t) + \int_{t}^{t+\Delta t} (\vec{v}(\vec{x}, \tau) + \vec{v_S}(\vec{x}, z, \tau))d\tau + R\sqrt{\frac{2dtK_h}{r}} \quad (1)$$

where $\vec{v}(\vec{x}, t)$ is the horizontal surface velocity at the particle location $\vec{x}(t)$ at time t, $\vec{v_S}(\vec{x}, z, \tau)$ is the horizontal Stokes drift, $R \in [-1, 1]$ is a random process representing subgrid motion with mean zero and variance $r = 1/3$, dt is the integration time step, and $K_h = 10\ m^2\ s^{-1}$ is the horizontal diffusion coefficient.[46,62] The depth-dependent horizontal Stokes drift is calculated based on Breivik et al.[8] Eq 1 is integrated using a fourth order Runge−Kutta scheme with $dt = 30$ s, and particle positions are saved every 12 h.

The turbulent vertical particle transport is modeled as a Markov-0 process following Onink et al.,[63] where the vertical particle position $z(t)$ is calculated by

$$z(t + \Delta t) = z(t) + (w_r + \partial_z K_z(\vec{x}, z, t))dt + \sqrt{2K_z(\vec{x}, z, t)}\, dW \quad (2)$$

where w_r is the particle rise velocity, $K_z(\vec{x}, z, t)$ is the vertical diffusion coefficient, $\partial_z K_z = \partial K_z/\partial z$, dW is a Wiener increment with zero mean and variance dt, and the vertical axis z is defined positively downward with $z = 0$ at the air-sea interface. Since the vertical and horizontal diffusion fields are not provided within the CMSPRP data set, we use a local form of the K-profile parametrization (KPP)[7,48] for the wind-driven vertical $K_{z,W}$ profile within the surface mixed layer

$$K_{z,W}(\vec{x}, z, t) = \left(\frac{\kappa u_{*w}(\vec{x}, t)}{\phi}\theta\right)(|z| + z_0)\left(1 - \frac{|z|}{MLD(\vec{x}, t)}\right) \quad (3)$$

where $\kappa = 0.4$ is the von Karman constant, $u_{*w}(\vec{x}, t) = \tau(\vec{x}, t)/\rho_w(\vec{x}, t)$ is the friction velocity of water, $\phi = 0.9$ is the stability function in Monin-Obuokov boundary layer theory, θ is the Langmuir circulation enhancement factor, and z_0 is the roughness scale of turbulence following[85] for a wave age $\beta = 1.21$.[45,63] Langmuir circulation (LC) turbulent mixing can increase turbulent mixing up to $\theta = 3$−4,[55] but as calculating θ is not trivial, we assume conservative wind mixing with negligible LC-driven mixing where $\theta = 1.0$. Following Large et al.[48] and Boufadel et al.,[7] we assume $K_{z,W}(\vec{x}, z, t) = 0$ for $z > MLD$. We also account for tidal-driven vertical mixing $K_{z,T}(\vec{x}, z, t)$ throughout the water column based on tidal mixing climatologies,[19] where the full vertical vertical mixing coefficient $K_z(\vec{x}, z, t)$ is expressed by

$$K_z(\vec{x}, z, t) = \begin{cases} \text{if } z \le \text{MLD}, K_z(\vec{x}, z, t) = K_{z,W}(\vec{x}, z, t) + K_{z,T}(\vec{x}, z, t) \\ \text{if } z > \text{MLD}, K_z(\vec{x}, z, t) = K_{z,T}(\vec{x}, z, t) \end{cases} \quad (4)$$

The particle rise velocity w_r depends on the particle size and for a spherical particle with diameter d is calculated as

$$w_r = \sqrt{\frac{\left(1 - \frac{\rho_p}{\rho_w(\vec{x}, z, t)}\right) \times 8/3 \times d \times g}{24/\mathrm{Re}(\vec{x}, z, t) + 5/\sqrt{Re(\vec{x}, z, t)} + 2/5}} \quad (5)$$

for the particle density ρ_p, seawater density ρ_w, gravitational acceleration $g = 9.81\ m\ s^{-2}$, and Reynolds number $Re(\vec{x}, z, t) = w_r d/\nu(\vec{x}, z, t)$ with the kinematic viscosity of seawater ν.[25] The kinematic viscosity $\nu(\vec{x}, z, t)$ at the particle position is calculated following ref 42.

Following Onink et al.,[63] the boundary condition at the ocean surface has the particle depth set at $z = 0$ if the particle crosses the air-surface interface. Microplastic entrainment remains a highly uncertain process, and there is insufficient field and laboratory data to properly parametrize seabed settling and entrainment. Therefore, a reflecting boundary condition is applied where a particle is reflected at the seabed without any possibility of settling or particle flux through the seabed.

The beaching and resuspension of particles on coastlines is modeled following Onink et al.[62] Concentrations of beached microplastics are influenced by a wide range of processes, such as winds, coastal morphology, tides, and human usage of the beach.[9,10,20,32,40,68,72] However, such processes typically act on smaller spatial and temporal scales than those resolved in

https://doi.org/10.1021/acs.est.2c03363
Environ. Sci. Technol. 2022, 56, 15528−15540

ocean reanalysis products. As such, particle beaching is implemented as a stochastic process where a particle's beaching probability p_B for time step dt is

$$p_B = \begin{cases} \text{if } d \le D,\ p_B = 1 - \exp(-dt/\lambda_B) \\ \text{if } d > D,\ p_B = 0 \end{cases} \quad (6)$$

where d is the distance from the particle to the nearest model land cell, D sets the outer limit of the beaching zone within which beaching is possible, and λ_B is the beaching time scale in days. Following Onink et al.,[62] we set the beaching zone D = 6 km such that all land-adjacent ocean cells are fully contained within the beaching zone. The probability p_R of beached particles being resuspended for a time increment dt is

$$p_R = 1 - \exp(-dt/\lambda_R(w_r)) \quad (7)$$

where the resuspension time scale $\lambda_R(w_r)$ is size-dependent. Based on field experiments with drifters of various sizes, Hinata et al.[34] found a linear relationship between the particle rise velocity and the resuspension time scale in days

$$\lambda_R(w_r) = 260 \times w_r + 7.1 \quad (8)$$

where smaller particles have smaller rise velocities and are more likely to be resuspended. While Hinata et al.[34] only considered a single beach in Japan, it is the only field study that has studied the relation between particle size and beach residence time, and therefore, we apply the relation to the Mediterranean. There is likely also a relation between the particle size and the beaching probability, but as this has not been sufficiently studied to date, we set λ_B to a uniform value of 26 days, based on the model calibration study in Kaandorp et al.[38] To prevent particles getting stuck on land cells, an antibeaching current is applied where particles within 500 m of a land cell are pushed back at 1 m s^{-1}.[62,64] This does not affect the relative large-scale distribution of particles[64] and assures beaching can only occur following eq 6. The order in which all parametrizations are applied is indicated in Figure S1.

2.3. Fragmentation Model. *2.3.1. Kaandorp Box Model and Ocean Fragmentation.* The fragmentation model is based on Kaandorp et al.,[39] where plastic particles split into smaller fragments based on fractal theory.[12,77] For a spatial dimension D_N = 3, one starts from a cubic parent object with dimensions L in size class k = 0. Over time this parent object splits into smaller fragments, where fragments in size class k = n have size $L/2^n$. The continuous fragmentation index f indicates the number of full fragmentation cycles that have taken place, where the probability mass function (pmf) gives the mass fraction m in each size class k

$$m(k; f, p) = \frac{\Gamma(k+f)}{\Gamma(k+1)\Gamma(f)} p^k (1-p)^f \quad (9)$$

where p is the fraction of the original parent object that has been lost to smaller size classes at f = 1, and Γ is the gamma function. For $k = \infty$, eq 10 has mass conservation, but with a finite number of size classes mass is gradually lost. The number of fragments $n(k, f, p)$ in each size class is

$$m(k; f, p) = \frac{\Gamma(k+f)}{\Gamma(k+1)\Gamma(f)} p^k (1-p)^f \quad (10)$$

where p is the fraction of the original parent object that has been lost to smaller size classes at f = 1, and Γ is the gamma function. For $k = \infty$, eq 10 has mass conservation, but with a finite number of size classes mass is gradually lost. The number of fragments $n(k, f, p)$ in each size class is

$$n(k, f, p) = 2^{D_N k} m(k; f, p) \quad (11)$$

While a spatial dimension of D_N = 3 indicates a cubic parent object, D_N = 2 corresponds to a sheet, and a noninteger D_N would indicate a mixture of various particle types. A value of p = 0.4 was reported to be suitable for pellets made out of polymers such as polyethylene and polypropylene. The fragmentation index f is related to the time an object spends in the maritime environment, but the fragmentation rate is highly uncertain. Laboratory experiments indicate a linear fragmentation rate of $1.8 \times 10^{-2} f$ week^{-1},[75] while fitting the fragmentation model to observational data of particle sizes suggested a rate of $2.0 \times 10^{-4} f$ week^{-1}.[39] Defining the fragmentation time scale λ_f as the time in days such that f = 1 (implying 40% mass loss of the parent object with p = 0.4), this implies λ_f = 388−35000 days.[39,75] However, this relation between f and time is not necessarily linear and likely varies depending on environmental conditions and the polymeter type.[2]

To study the microplastic fragmentation in the Mediterranean, Kaandorp et al.[39] developed a box model representing microplastic transport between beaches, coastal waters, and open water for various particle size classes. The transition probabilities between the coastal and open waters are based on Lagrangian simulations using the same CMSPRP and MSWR data products used in this study,[38] while the particle resuspension followed eq 8. Kaandorp et al.[39] also assumed that fragmentation only occurs on beaches. For the full details of the implementation of the box model, we refer to Kaandorp et al.[39] In order to test the sensitivity of the box model to ocean fragmentation, we modify the box model to also allow for fragmentation in coastal and open waters. We therefore differentiate between the beach-based fragmentation time scale $\lambda_{f,B}$ and the coastal/open water fragmentation time scale $\lambda_{f,O}$.

Kaandorp et al.[39] included a sink term P_S in the box model, such that the amount of plastics in the ocean system steady state matched observed plastic quantities. The steady state concentrations in the beach and coastal/open water reservoirs can then be solved by matrix inversion, where depending on the fragmentation rate a steady state is reached after approximately a decade of simulation time.

The sensitivity analysis of ocean fragmentation considers a base scenario with only beach-based fragmentation particles in 12 size classes (d = 0.002−5.000 mm) with $\lambda_{f,B} \in$ [388, 35000]days. We then add coastal/open water fragmentation with $\lambda_{f,O} \in [1, 5, 10, 100, 1{,}000, 10{,}000] \times \lambda_{f,B}$. We assume a continuous weekly microplastic input of size class k = 0 for the purpose of the sensitivity analysis. We set λ_B = 26 days[38] and λ_R according to eq 8.

2.3.2. Lagrangian Model. The Kaandorp et al.[39] fragmentation model predicts an exponential rise in the number of microplastic fragments in the system. Given that it is not computationally feasible to represent each microplastic fragment with an individual virtual particle, each virtual particle represents a certain microplastic number/mass within a given size class. In addition, the generation of fragments is discretized instead of being continuous and gradual.

For illustration, consider a virtual particle which represents microplastic particles in the k = 0 size class (d = 5.000 mm) with an initial number and mass weight of 1. When this particle

https://doi.org/10.1021/acs.est.2c03363
Environ. Sci. Technol. 2022, 56, 15528−15540

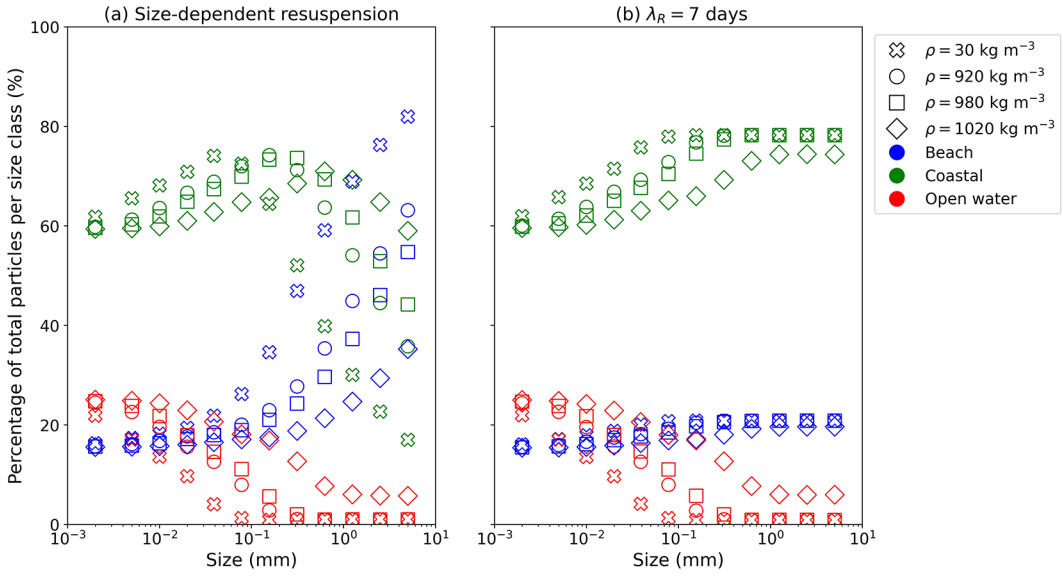

Figure 1. Mediterranean beach (blue symbols), coastal (green), and open water reservoirs (red) as percentages of the total number of particles in each size class and in each microplastic density for (a) size-dependent resuspension and (b) size-independent resuspension time scale λ_R = 7 days. The fractions are averaged over the entire three year simulations. Each size class/particle density represents an individual model simulation.

is released, its horizontal and vertical transport is calculated by eqs 1 and 2, and it cycles through beaching and resuspension. Assuming that fragmentation only occurs when a particle is beached, a timer tracks the cumulative time that the particle is beached (even if it is resuspended intermittently). Once this timer indicates that a particle has been beached for 90 days, it fragments, and 5 new particles are created corresponding to size classes k = 1−5. Based on the fragmentation time scale λ_f, the beached time converts to the equivalent fragmentation index f, which in turns sets the particle number and mass for each of the virtual particles based on eqs 10 and 11. The beach timer then resets, with all newly created particles being initially beached at the same location as the parent particle.

The described procedure applies to all particles in our fragmentation scenario (e.g., fragmentation of a k = 2 particle can create k = 3−5 fragments), where we track particles for up to 3 years with $\lambda_f \in$ [388, 1000, 10000, 35000, 50000] days. In the Lagrangian fragmentation scenario, we only consider 6 size classes (d = 0.156−5.000 mm) with ρ = 920 kg m^{-3}, both due to computational constraints and since our fragmentation validation rests almost solely on Neuston net measurements, which generally have a mesh size of 0.33 mm. Any particle mass transfer to smaller size classes (d < 0.156 mm) is considered lost from the system.

2.4. Lagrangian Model Input. For all simulations, the spatial distribution of microplastic inputs is scaled according to riverine inputs,[50] where particles are released in shore-adjacent ocean cells. For each particle size in the size-dependent transport scenario, we release 85,196 particles at the beginning of the simulation. Since the size-dependent transport scenarios do not have an exponential increase in the number of particles, we consider 12 size classes (d = 0.002−5.000 mm) with particle densities $\rho \in$ [30, 920, 980, 1020] kg m^{-3}, which correspond to expanded polystyrene (PS), polypropylene (PP), polyethylene (PE), and approximately neutrally buoyant polymers.[9] With the fragmentation scenarios, we release 2718 particles per month (97,848 in total), where these are evenly divided over the six size classes. The initial weighing of the particles across the size classes is based on river microplastic size distributions.[84] While the size distribution of microplastics entering the ocean can vary in space and time,[50,74,84] we lack the necessary field data to represent such input variability and assume temporal and spatial invariance in the input size distribution.

All simulations in both the size-dependent transport and fragmentation scenarios ran for three years (2010−2012). While this is insufficient time for the system to reach any equilibrium in the fragmentation scenarios, the exponential increase in the number of virtual particles with each additional simulation year means that longer simulations are computationally infeasible. However, three years is sufficient to study the horizontal and vertical spread of microplastics throughout the Mediterranean and to quantify the mass loss rate of microplastics due to fragmentation.

3. RESULTS

3.1. Size-Dependent Transport. Figure 1 shows the relative distribution of particles between beaches, coastal waters (<10 km from the model coastline), and open water (>10 km from the model coastline), where each simulation corresponds to a given particle size and density averaged over 3 years. Almost all the large (d = 5.000 mm) particles are near coastlines, either beached (35.24−81.96%, depending on the density) or adrift in the coastal zone (17.01−59.01%), with only a small fraction in open water (1.04−5.74%). For the smallest particles (d = 0.002 mm), the open water fraction rises to 21.85−25.08%, with the coastal zone holding the majority of the particles (59.37−61.84%). Microplastic particles are less likely to be beached as the particle size decreases, as smaller rise velocities result in shorter resuspension time scales. However, with the exception of the ρ = 30 kg m^{-3} particles, only around 1% of particles reach open water for sizes d > 0.156 mm, as particles remain close to land. While the exact distribution of particles over the beached, coastal, and open water slightly varies with particle density, the general trends with decreasing size are the same. The near-shore trapping of almost all microplastics d > 0.1 mm also occurs with size-independent resuspension (Figures 1b and S2).

https://doi.org/10.1021/acs.est.2c03363
Environ. Sci. Technol. 2022, 56, 15528−15540

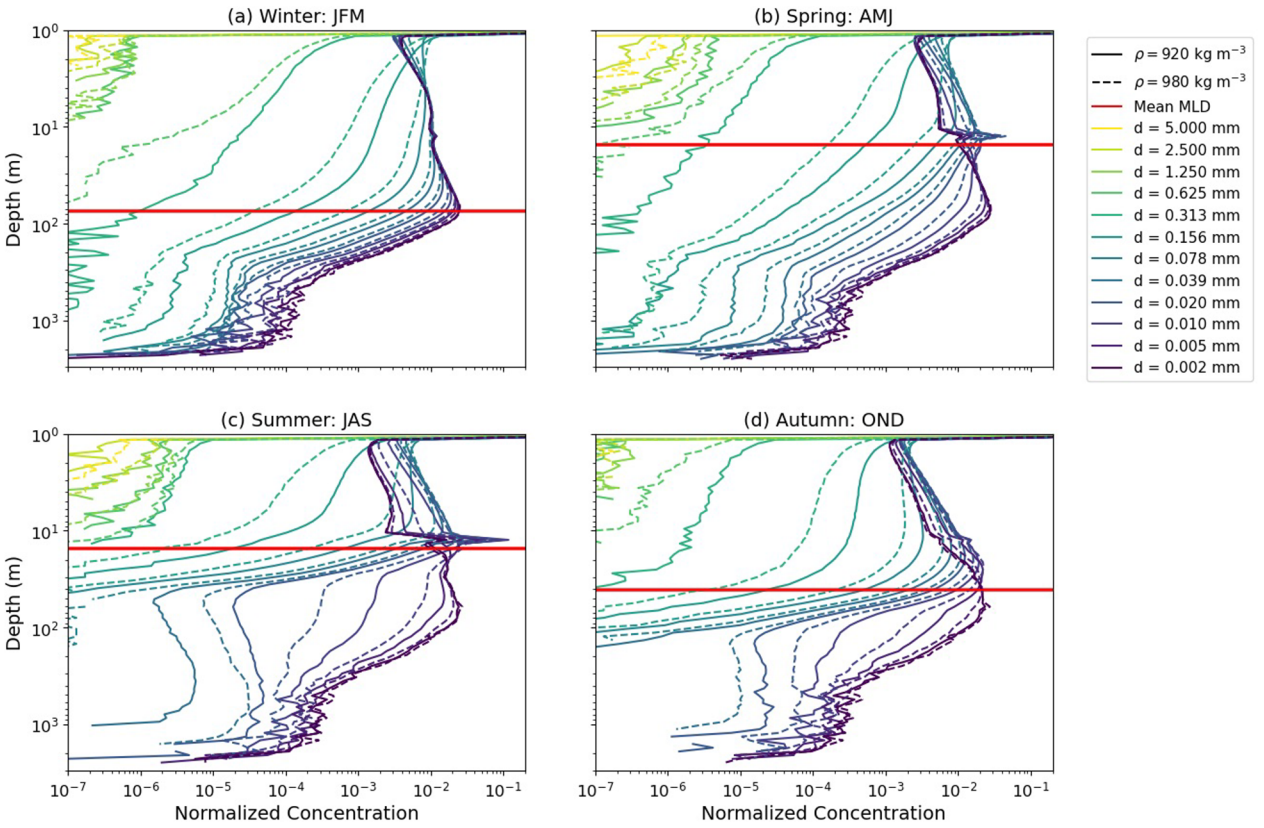

Figure 2. Normalized vertical microplastic concentrations during different seasons and for 5.000−0.002 mm particles with $\rho \in [920, 980]$ kg m^{-3} with size-dependent resuspension. All profiles are averaged over the three year simulation period and normalized by the total number of particles in each simulation (n = 85, 196).

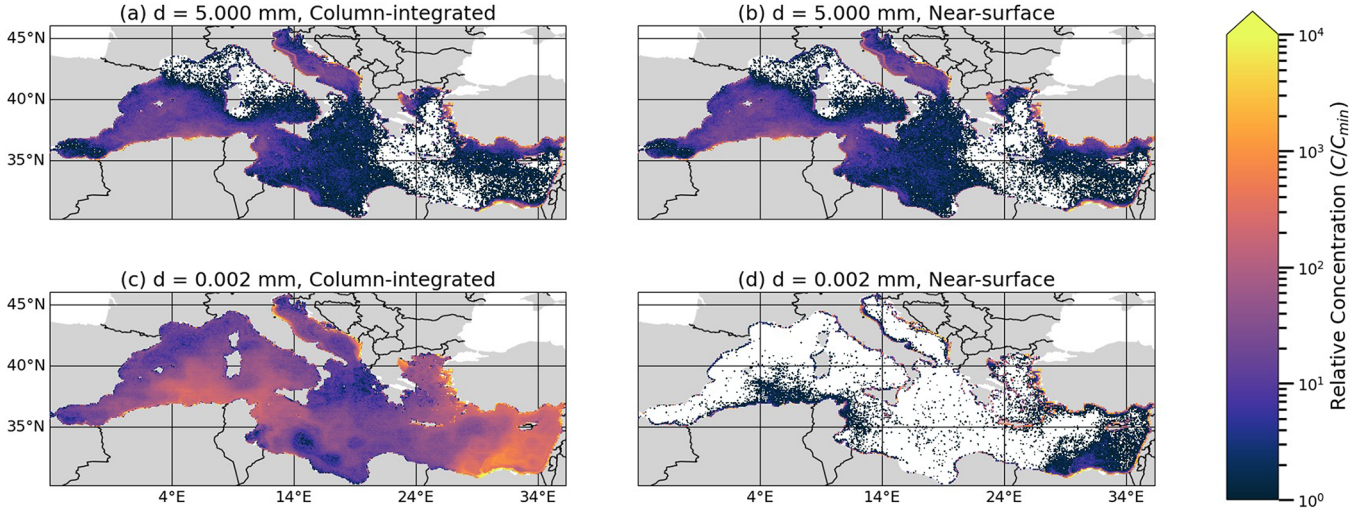

Figure 3. Column-integrated and near surface (particle depth z < 1 m) horizontal microplastic concentrations for (a - b) 5.0 mm and (c - d) 0.002 mm particles. All concentrations represent the first year of the simulation with size-dependent resuspension and ρ = 920 kg m^{-3}.

The near-shore trapping of microplastics depends on local circulation patterns, and the likelihood of microplastics to reach the open ocean varies spatially (Figure S3). While certain areas, such as the western Mediterranean coastlines, show relatively little near-shore trapping for any particle size, generally small particles are more likely to reach the open ocean than large particles. However, certain regions such as the Adriatic Southern Italian coastline show the opposite trend where larger particles are more likely to reach the open ocean.

The vertical and horizontal distributions are strongly affected by the particle size. Smaller and denser microplastic particles are mixed deeper below the ocean surface (Figures 2 and S4), where up to 58.21% of the smallest and heaviest microplastics are below 10 m from the ocean surface (Table S1). The vertical transport of particles varies seasonally, as stronger stratification during the spring and summer months generally leads to shallower mixing (Figure 3 and Table S1). However, vertical mixing by internal tides can transport

https://doi.org/10.1021/acs.est.2c03363
Environ. Sci. Technol. 2022, 56, 15528−15540

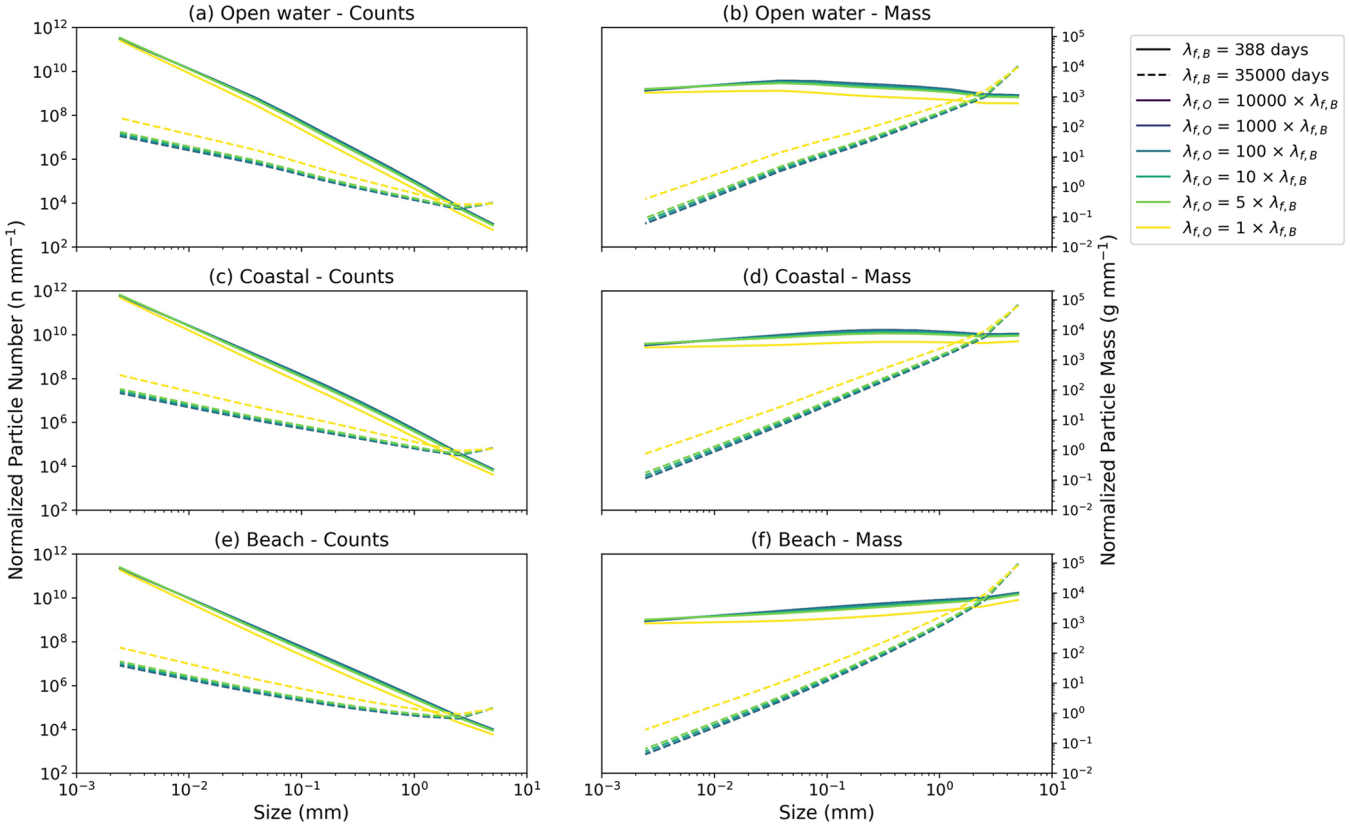

Figure 4. Steady-state normalized microplastic size distributions of microplastic particles with varying beach and ocean fragmentation time scales using the Kaandorp et al.[39] box model.

particles down far below the MLD, with particles of various sizes and densities reaching over 2,000 m below the ocean surface.

In summary, large particles remain at the ocean surface, whereas smaller particles can get mixed far below the ocean surface; and this is reflected in the horizontal distribution. The open water column-integrated concentrations are orders of magnitude lower for large (d = 5.000 mm) (Figures 3a and S5) rather than small (d = 0.002 mm) particles (Figures 3c and S5) in the first simulation year. This is in large part due to larger particles being more likely to beach and less likely to reach open water. The horizontal distribution is strongly dependent on the input scenario, with the highest concentrations near the Algerian coast and in the Levantine Sea. However, by the third simulation year the smaller (d < 0.078 mm) particles are distributed more homogeneously throughout the entire Mediterranean basin (Figure S6g-l), while almost all larger (d > 0.078 mm) particles are either beached or in coastal areas (Figure 6a-f). However, as smaller microplastic particles are more easily mixed below the surface, the near-surface microplastic concentrations are higher for large rather than small particles (Figures 3b and d, S7, and S8). As such, while smaller microplastic particles are more likely to reach open waters in the Mediterranean, our model suggests they are less likely to be observed in surface water. Surface field measurements similarly show relatively low surface concentrations of small (<1 mm) microplastics,[15,31,71] which is likely due to a combination of the ocean dynamics demonstrated in this model and difficulties in sampling small microplastic particles.

3.2. Ocean Fragmentation. We next examine the effect of fragmentation on the size distribution of microplastic particles with the Kaandorp box model. Figure 4 shows the steady-state size distributions assuming different ocean-based fragmentation time scales $\lambda_{f,O}$, separated into open water, coastal, and beach reservoirs. The baseline steady state size distributions show an exponential increase in the number of particles for smaller size classes. The faster beach fragmentation time scale $\lambda_{f,B}$ = 388 days results in 4 orders of magnitude more particles and mass in smaller size classes compared to $\lambda_{f,B}$ = 35,000 days. The addition of ocean fragmentation has a minimal influence on the modeled size distribution unless $\lambda_{f,O} \approx \lambda_{f,B}$, i.e., ocean fragmentation is equally fast as fragmentation on beaches.

Based on laboratory experiments, the ocean fragmentation time scale $\lambda_{f,O}$ is highly variable and dependent on the object polymer, object type, and experimental setup (Table 1). Assuming a fragmentation fraction p = 0.4, a parent object would lose 40% of its initial mass over a full fragmentation cycle (f = 1), and this is estimated to take anywhere from years to centuries in marine environments. However, for the type of PP and PE fragments considered in this study, $\lambda_{f,O}$ appears to be on the order of decades. Compared with the $\lambda_{f,B}$ estimates from ref 75 of 0.3−1.1 years, this would suggest that ocean-based fragmentation is negligible relative to beach-based fragmentation, at least within the Mediterranean. We acknowledge however that laboratory fragmentation estimates do not include interactions of microorganisms with particles and hence may underestimate open-ocean fragmentation rates.

3.3. Lagrangian Fragmentation. Based on the sensitivity study performed with the box model, we solely consider beach-based fragmentation in our Lagrangian fragmentation scenario, and λ_f henceforth refers to the beach-based fragmentation time scale $\lambda_{f,B}$. Three simulation years is insufficient for a steady

https://doi.org/10.1021/acs.est.2c03363
Environ. Sci. Technol. 2022, 56, 15528−15540

Table 1. Estimates of the Ocean-Based Fragmentation Time Scale $\lambda_{f,O}$ from Literature Sources[a]

study	plastic object	$\lambda_{f,O}$
O'Brine and Thompson[60]	PE strip	15.3−19.2 years[b,c]
	compostable polyester strip	<0.5 years[b,c]
Resmerită et al.[70]	PP strip	20.2−25.8 years
Zhu et al.[87]	postconsumer expanded PS fragment	0.3−2.7 years[c]
	postconsumer PP fragment	0.3−4.3 years[c]
	postconsumer PE fragment	33 years[c]
	PE pellet	0.5−49 years[c]
	North Pacific Gyre (NPG) fragments	2.8 years[c]
	NPG fragments (no UV)	58 years[c]
Gerritse et al.[30]	low-density PE air pouch	50−63.6 years
	high-density PE air pouch	66.6−84.9 years
	PS packaging foam	33.3−42.3 years
	PS beaker	400.0−510.6 years
	Latex balloon	8.7−10.8 years
	silicon tube	40.0−50.8 years
	PET bottle	8.2−14.3 years
	PET fleece	13.8−17.4 years
	PU foam	13.3−16.8 years
	cellulose beaker	5.1−6.2 years
	CA cigarette filter	2.7−3.2 years
	compostable postal bag	2.6−3.1 years
	compostable trash bag	1.5−1.6 years
	PLA food bag	5.6−6.9 years

[a]Unless otherwise noted, the lower and upper bounds are estimates of the time for the parent object to lose 40% of its original mass assuming linear and exponential mass loss rates. [b]Assumes the loss of the strip surface area is equivalent to the loss of mass. [c]Estimate of the time scale for the parent object to lose all mass provided directly by the literature source.

state to be established, and the size distributions are heavily influenced by the initial input size distribution (Figure 5). It is only in the smallest size classes that clear differences arise between the various λ_f values. The fragmentation with λ_f = 388 days is over 2 orders of magnitude faster than with λ_f = 50,000 days, and in the coastal and beached reservoirs, the k = 5 size class correspondingly has 2 orders of magnitude more particles and mass. However, in the open water, these differences are smaller due to the relatively small number of particles reaching open water. There is a gradual mass transfer to smaller size classes, but the overall mass loss to size classes < 0.156 mm (smaller than the regular Neuston net mesh size) is only 0.24−2.45%.

The horizontal spread of the microplastic size classes resembles the distribution in the size-dependent transport scenarios (Figures 3 and 6), with the concentrations near coastlines being orders of magnitude higher than in the open ocean. Smaller size classes generally show higher concentrations in open water due to the shorter resuspension time scales and decreased coastal trapping. However, although smaller particles are more numerous (Figure 6), the larger size classes still hold a large portion of the total microplastic mass (Figure S9). For example, with λ_f = 388 days, by count 53.25% of the particles have a size d = 0.156 mm, but only 1.98% of the microplastic mass is in the size class (assuming spatial dimension D_N = 2.5). In contrast, the three largest size classes make up only 5.61% of the microplastic particles by count but 76.04% of the mass.

4. DISCUSSION

The distinct differences in the column-integrated and near-surface concentrations highlight the importance in considering the full 3D transport of microplastics. Particles with near-zero rise velocities, either due to their small size or being nearly neutrally buoyant relative to the seawater, are more likely to be mixed below the ocean surface.[36] As suggested by Cózar et al.,[14] this can be a partial explanation of why microplastic measurements collected with Neuston nets show fewer small particles than expected. The near-surface concentration distribution in the first model year closely resembles that of Tsiaras et al.,[76] despite using a different input scenario and model setup. For the larger size classes (d > 0.313 mm), this also matches well with field measurements throughout the Mediterranean basin.[15,66] However, validating the horizontal distribution of particles smaller than ≈0.1−0.33 mm is currently not possible, as these particles are generally not captured within Neuston nets and alternative sampling methodologies are not commonly used. Similarly, while the high subsurface concentrations predicted by the model are in line with observations,[24,65,67,69] these observational records do not have sufficiently high temporal and spatial resolutions to validate the modeled vertical concentration profiles. This would also require sampling techniques other than Neuston nets, such as Niskin bottles[67] or high-volume filtration systems,[86] to study the distribution of microplastic particles < 0.33 mm.

The transformation of microplastic particles due to fragmentation is critical for understanding the long-term fate of microplastics, as changes in the particle size can affect the large-scale transport and the bioavailability to marine ecosystems. While various processes and properties are known to affect the fragmentation rate, such as polymer type, UV exposure, and oxidation,[75] isolating which is the dominant process is vital for developing basic fragmentation models. One simplifying assumption made by Kaandorp et al.[39] was that fragmentation predominantly occurred on beaches, and based on the results in this current study and Isobe and Iwasaki,[37] this assumption appears justified. While comparing fragmentation rates from different experimental setups is challenging, the fragmentation time scale for polyethylene and polypropylene polymers is generally on the order of decades in water, compared to years in a beach-like environment.[75] As such, neglecting ocean-based fragmentation likely will have a negligible impact on the results on this study. However, for other plastic polymers outside of the immediate scope on this study, such as cellulose, PLA, and compostable polymers, $\lambda_{f,O}$ appears to be on the order of years, and neglecting ocean-based fragmentation may result in underestimating the fragmentation of such plastic objects.

Over a three year period, fragmentation is not shown to lead to significant amounts of lost microplastic mass, as the mass transfer to size classes d < 0.156 mm is at most 2.45%. In reality, this mass fraction loss is probably even smaller, as most plastic mass would be contained in objects larger than the 5 mm particles considered in this modeling study. Given the slow rate at which microplastic fragmentation occurs, after three years, the modeled size distributions still closely resemble the input size distribution. As such, greater understanding of the size distribution of microplastic inputs would provide

https://doi.org/10.1021/acs.est.2c03363
Environ. Sci. Technol. 2022, 56, 15528−15540

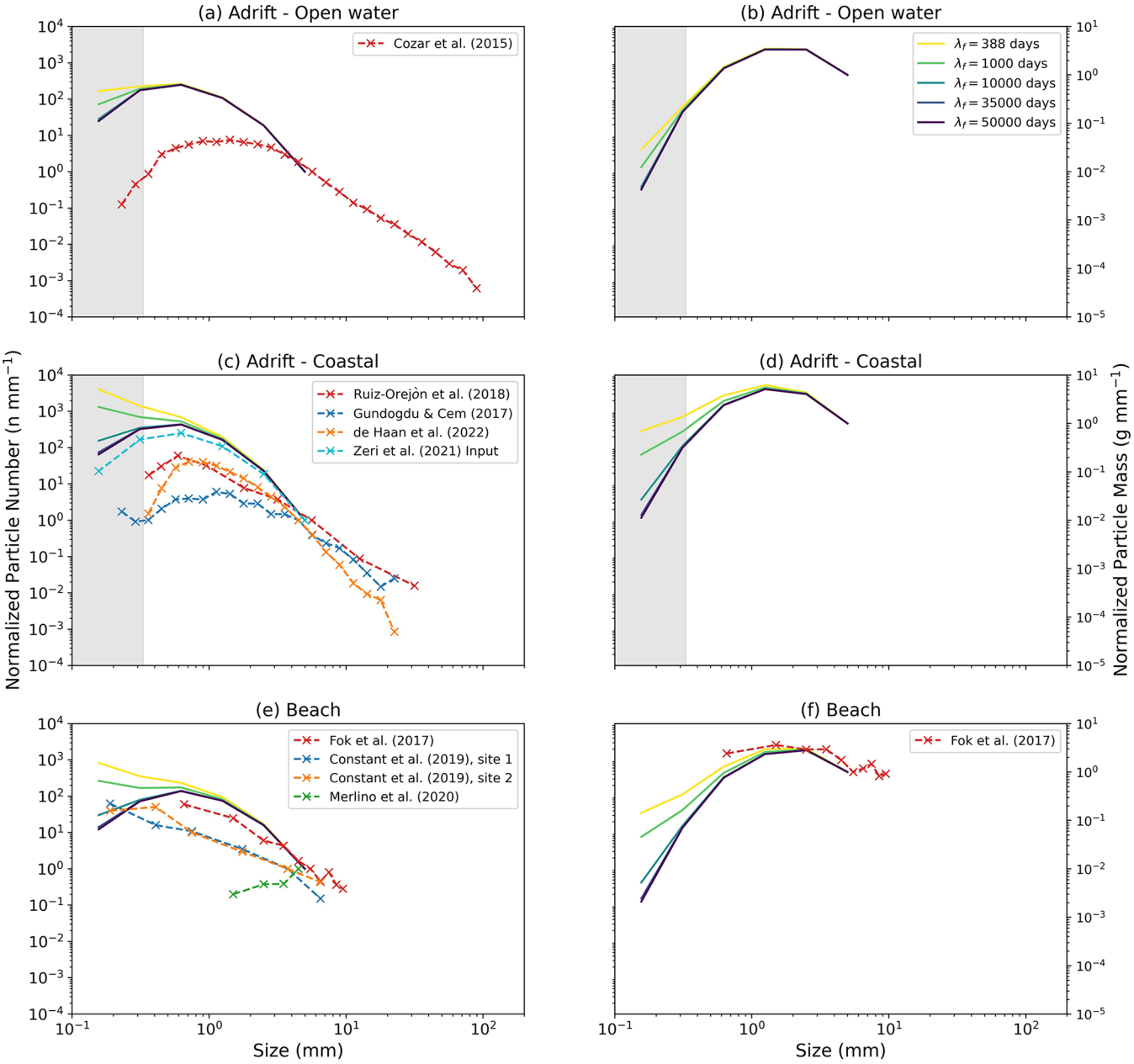

Figure 5. Comparisons of the surface (<0.26 m) Lagrangian modeled and measured microplastic size distributions (MSDs). All modeled MSDs are normalized to the maximum size class, and all measured MSDs are normalized relative to the measured size class closest to 5 mm. The Zeri et al.[84] data in panel (c) indicates the size distribution of particles entering the simulation. In panels (a - d), the gray-shaded area indicates particle sizes < 0.33 mm, representing particle sizes below the detection limits of typical Neuston nets used to collect surface microplastics.

insight into the size distribution of microplastics in the Mediterranean as a whole. Compared to size distributions from field measurements, the model predicts relatively higher amounts of microplastics in size classes k = 0−5. In part, this could be due to the lack of microplastic particles larger than d = 5.000 mm in the model, which could affect the relative number of particles in each size class. However, it is also possible that three years is simply not long enough for the model to stabilize to a long-term size distribution. However, the current Lagrangian model setup provides insight into the distribution of the microplastic fragments in the Mediterranean which is not possible with simpler box models. While observational studies often report microplastic concentrations as particle counts (e.g., Figure 5), it is shown in Figures 6 and S9 that microplastic mass and counts show different relative distributions. The number concentration of microplastics is dominated by smaller particles, but the distribution of microplastic mass is more strongly influenced by the distribution of larger particles. This difference could have important consequences for, e.g., quantifying risks associated with microplastic pollution.

Considering the results of both the size-dependent transport and Lagrangian fragmentation scenario, the fate of microplastics when they enter the Mediterranean is strongly size-dependent. Large microplastics tend to remain close to shore, where they are likelier to beach and gradually fragment into smaller particles. Eventually, as the particles get smaller and especially for particles $d \approx 0.156$ mm or smaller, particles are

https://doi.org/10.1021/acs.est.2c03363
Environ. Sci. Technol. 2022, 56, 15528−15540

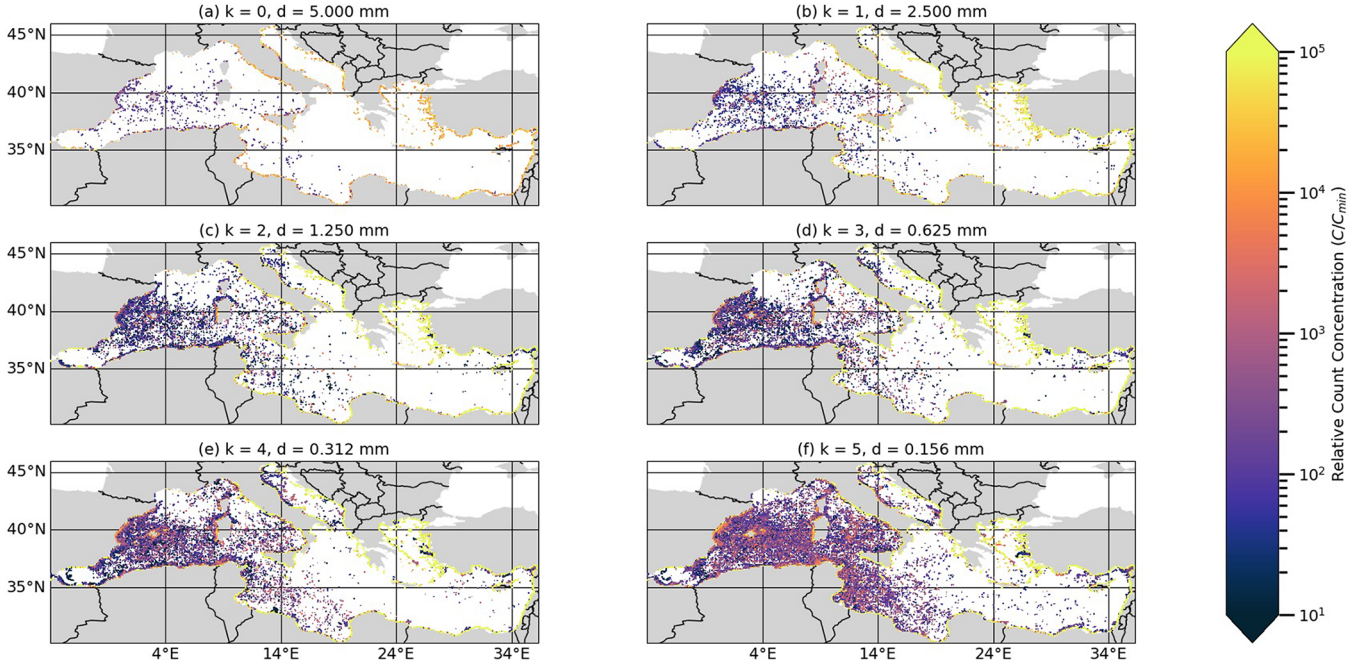

Figure 6. Columnn-integrated horizontal microplastic count concentrations for size classes $k = 0-5$ in the third simulation year.

likelier to reach open water. At this point, the particles are also sufficiently small so that vertical transport processes become more important, leading to greater mixing of the particles throughout the water column. Overall, this study reiterates the importance of coastal regions in the overall fate of microplastics suggested by Onink et al.[62] Given that many coastal processes occur on spatial and temporal time scales that are unresolved by large-scale circulation models such as CMSPRP and MSWR,[79] it is possible that such coastal trapping is weaker when all near-shore processes are represented. This still highlights an urgent need for greater understanding of the nearshore microplastic transport.[1,41] However, it is promising that the model shows the same size-dependent trapping pattern as Morales-Caselles et al.,[58] who found that larger debris appears more likely to remain trapped close to shore than smaller debris.

We consider a range of size-dependent processes, which have various degrees of uncertainty. There are numerous studies that calculate the rise velocity of a particle based on its density and size,[42,73,81] but the Enders et al.[25] parametrization was used due to relative computational ease within this model setup. However, depending on a particle's particular shape or spatial orientation, we acknowledge the rise velocity could vary.[13,22] There is higher uncertainty in the size-dependent resuspension time scale and similarly in assuming size-independent beaching time scales. The resuspension time scale is based on empirical experiments by Hinata et al.,[34] but the relation is an extrapolation for microplastic particles, as Hinata et al.[34] used drifters > 1.3 cm in size. However, size-independent resuspension time scales $\lambda_R \in [7, 50]$ days only affected the relative distribution of particles over the beached and coastal reservoirs, with the percentage of particles reaching open water remaining unaffected. Similarly, we assumed a single beaching time scale $\lambda_B = 26$ days for the entire Mediterranean, while this likely varies depending on the particle characteristics and local geomorphology. Given that the beaching time scale remains uncertain for any type of particle,[37,62] we used $\lambda_B = 26$ days based on an inverse modeling study that best fit with field measurements in the Mediterranean.[38] Furthermore, given that spatially varying beaching and resuspension time scales do not seem to affect the large-scale distribution of microplastic particles,[17] assuming spatial invariance in these time scales is the best available option until additional field experiments have been conducted.

Another assumption in the current model setup is that the particle density remains unchanged over the three year simulation period. Biofouling was not included in this study in order to focus solely on the influence of particle size. However, even without biofouling, microplastic particles are shown to be mixed throughout the entire water column, including down the seabed up to 3000 m deep. The size-dependent scenarios show this is even the case for particles up to 5 mm in size if the particle is nearly neutrally buoyant (Table S1). Yet, by excluding biofouling, the current study could be underestimating the amount of subsurface microplastics.[29] The amount of vertical mixing might also be underestimated by assuming negligible LC-driven mixing. The KPP wind mixing parametrization can account for LC-driven turbulence through the LC enhancement factor θ, but computing θ from spatially and temporally coarse reanalysis data is not trivial and beyond the scope of this study. Ideally, the CMSPRP data set would include vertical turbulent mixing data, as the Onink et al.[63] parametrization now had to use the MLD data from the CMSPRP data set. Since the MLD in the CMSPRP data set is defined by a density criteria relative to the seawater density at 10 m, during the spring and summer months, almost the entire Mediterranean basin had an MLD = 10 m, resulting in the artificial spike at $z = 10$ m in the vertical microplastic concentration profiles (Figure 2). However, with no readily available alternative parametrization for wind mixing that does not have its own set of limitations, this is the best possible approach.

The size-dependent modeling framework includes several complex physical processes that are not fully understood. Additional laboratory and modeling studies are required to advance our understanding of microplastic transport in the

https://doi.org/10.1021/acs.est.2c03363
Environ. Sci. Technol. 2022, 56, 15528−15540

ocean. While the seafloor potentially holds millions of tons of plastic debris,[4] the current understanding of microplastic settling and entrainment is insufficient to realistically account for these processes within large-scale models. With regards to fragmentation, more laboratory and ideally field experiments are required to measure the rate at which different polymers fragment in both beach and open ocean environments, preferably over a range of climatological environments. The current model framework also assumed simple relations between particle size, particle beaching, resuspension, and rise velocities, which should be refined in future studies. Finally, we reiterate the absolute necessity for more extensive and standardized sampling of microplastics in various marine environments, such that the observational record can be used to validate and constrain future modeling studies.

■ ASSOCIATED CONTENT

Supporting Information

The Supporting Information is available free of charge at https://pubs.acs.org/doi/10.1021/acs.est.2c03363.

Additional figures and table of insight into distribution and transport behavior of microplastic particles with different sizes and densities and schematic of all model components for calculating 3D particle trajectory (PDF)

■ AUTHOR INFORMATION

Corresponding Author

Victor Onink − *Climate and Environmental Physics, Physics Institute, University of Bern, 3012 Bern, Switzerland; Oeschger Centre for Climate Change Research, University of Bern, 3012 Bern, Switzerland; Institute for Marine and Atmospheric Research, Utrecht University, 3584CC Utrecht, The Netherlands;* orcid.org/0000-0003-4177-9893; Email: victor.onink@unibe.ch

Authors

Mikael L. A. Kaandorp − *Institute for Marine and Atmospheric Research, Utrecht University, 3584CC Utrecht, The Netherlands;* orcid.org/0000-0003-3744-6789

Erik van Sebille − *Institute for Marine and Atmospheric Research, Utrecht University, 3584CC Utrecht, The Netherlands;* orcid.org/0000-0003-2041-0704

Charlotte Laufkötter − *Climate and Environmental Physics, Physics Institute, University of Bern, 3012 Bern, Switzerland; Oeschger Centre for Climate Change Research, University of Bern, 3012 Bern, Switzerland*

Complete contact information is available at: https://pubs.acs.org/10.1021/acs.est.2c03363

Author Contributions

Development of the size-dependent transport scenario was done by V.O., with input from M.L.A.K., E.v.S., and C.L. Adapting the Kaandorp et al.[39] box model to the Lagrangian fragmentation scenario was done by V.O. and M.L.A.K., with input from C.L. The manuscript was written by V.O. and C.L., with extensive input from E.v.S. and M.L.A.K. All of the authors contributed to the overall study design and discussion of the analysis, with V.O. carrying out the analysis.

Notes

The authors declare no competing financial interest.

Code Availability. The model code is available at Onink.[61]

■ ACKNOWLEDGMENTS

Calculations were performed on UBELIX (www.id.unibe.ch/hpc), the HPC cluster at the University of Bern. V.O. and C.L. acknowledge support from the Swiss National Science Foundation (Project PZ00P2_174124 Global interactions between microplastics and marine ecosystems). E.v.S. and M.L.A.K. were supported by the European Research Council (ERC) under the European Union's Horizon 2020 research and innovation programme (Grant Agreement No. 715386). We would like to thank William de Haan, Anna Sànchez Vidal, Christina Zeri, Sedat Gündoğdu, and Silvia Merlino for providing field measurements.

■ ABBREVIATIONS

CMSPRP, CMEMS Mediterranean Sea Physics Reanalysis Product; OGCM, ocean general circulation model; MSWR, Mediterranean Sea Waves Reanalysis; LC, Langmuir circulation; MLD, mixed layer depth; KPP, K-profile parametrization; pmf, probability mass function; PS, polystyrene; PE, polyethylene; PP, polypropylene

■ REFERENCES

(1) Alsina, J. M.; Jongedijk, C. E.; van Sebille, E. Laboratory measurements of the wave-induced motion of plastic particles: Influence of wave period, plastic size and plastic density. *Journal of Geophysical Research: Oceans* **2020**, *125* (12), e2020JC016294.

(2) Andrady, A. L. The plastic in microplastics: A review. *Marine pollution bulletin* **2017**, *119* (1), 12−22.

(3) Ballance, A.; Ryan, P.; Turpie, J. How much is a clean beach worth? The impact of litter on beach users in the Cape Peninsula, south africa. *South African Journal of Science* **2000**, *96* (5), 210−230.

(4) Barrett, J.; Chase, Z.; Zhang, J.; Holl, M. M. B.; Willis, K.; Williams, A.; Hardesty, B. D.; Wilcox, C. Microplastic pollution in deep-sea sediments from the great australian bight. *Frontiers in Marine Science* **2020**, *7*, 576170.

(5) Beaumont, N. J.; Aanesen, M.; Austen, M. C.; Börger, T.; Clark, J. R.; Cole, M.; Hooper, T.; Lindeque, P. K.; Pascoe, C.; Wyles, K. J. Global ecological, social and economic impacts of marine plastic. *Marine pollution bulletin* **2019**, *142*, 189−195.

(6) Bergmann, M.; Wirzberger, V.; Krumpen, T.; Lorenz, C.; Primpke, S.; Tekman, M. B.; Gerdts, G. High quantities of microplastic in arctic deep-sea sediments from the hausgarten observatory. *Environ. Sci. Technol.* **2017**, *51* (19), 11000−11010.

(7) Boufadel, M.; Liu, R.; Zhao, L.; Lu, Y.; Özgökmen, T.; Nedwed, T.; Lee, K. Transport of oil droplets in the upper ocean: impact of the eddy diffusivity. *Journal of Geophysical Research: Oceans* **2020**, *125* (2), e2019JC015727.

(8) Breivik, Ø.; Bidlot, J.-R.; Janssen, P. A. A stokes drift approximation based on the phillips spectrum. *Ocean Modelling* **2016**, *100*, 49−56.

(9) Brignac, K. C.; Jung, M. R.; King, C.; Royer, S.-J.; Blickley, L.; Lamson, M. R.; Potemra, J. T.; Lynch, J. M. Marine debris polymers on main hawaiian island beaches, sea surface, and seafloor. *Environ. Sci. Technol.* **2019**, *53* (21), 12218−12226.

(10) Browne, M. A.; Chapman, M. G.; Thompson, R. C.; Amaral Zettler, L. A.; Jambeck, J.; Mallos, N. J. Spatial and temporal patterns of stranded intertidal marine debris: is there a picture of global change? *Environ. Sci. Technol.* **2015**, *49* (12), 7082−7094.

(11) Carlson, D. F.; Suaria, G.; Aliani, S.; Fredj, E.; Fortibuoni, T.; Griffa, A.; Russo, A.; Melli, V. Combining litter observations with a regional ocean model to identify sources and sinks of floating debris in a semi-enclosed basin: the adriatic sea. *Frontiers in Marine Science* **2017**, *4*, 78.

(12) Charalambous, C.*On the evolution of particle fragmentation with applications to planetary surfaces*; 2014; DOI: 10.25560/32780.

(13) Clark, L. K.; DiBenedetto, M. H.; Ouellette, N. T.; Koseff, J. R. Settling of inertial nonspherical particles in wavy flow. *Physical Review Fluids* **2020**, *5* (12), 124301.
(14) Cózar, A.; Echevarría, F.; González-Gordillo, J. I.; Irigoien, X.; Úbeda, B.; Hernández-León, S.; Palma, Á. T.; Navarro, S.; García-de Lomas, J.; Ruiz, A.; Fernández-de Puelles, M. L.; Duarte, C. M. Plastic debris in the open ocean. *Proc. Natl. Acad. Sci. U. S. A.* **2014**, *111* (28), 10239−10244.
(15) Cózar, A.; Sanz-Martín, M.; Martí, E.; González-Gordillo, J. I.; Ubeda, B.; Gálvez, J. Á.; Irigoien, X.; Duarte, C. M. Plastic accumulation in the mediterranean sea. *PloS one* **2015**, *10* (4), e0121762.
(16) Critchell, K.; Grech, A.; Schlaefer, J.; Andutta, F.; Lambrechts, J.; Wolanski, E.; Hamann, M. Modelling the fate of marine debris along a complex shoreline: Lessons from the great barrier reef. *Estuarine, Coastal and Shelf Science* **2015**, *167*, 414−426.
(17) Daily, J.; Onink, V.; Jongedijk, C. E.; Laufkötter, C.; Hoffman, M. J. Incorporating terrain specific beaching within a lagrangian transport plastics model for lake erie. *Microplastics and Nanoplastics* **2021**, *1* (1), 19.
(18) de Haan, W. P.; Uviedo, O.; Ballesteros, M.; Canales, Í.; Curto, X.; Guart, M.; Higueras, S.; Molina, A.; Sanchez-Vidal, A. The Surfing for Science Group, Floating microplastic loads in the nearshore revealed through citizen science. *Environmental Research Letters* **2022**, *17* (4), 045018.
(19) de Lavergne, C.; Vic, C.; Madec, G.; Roquet, F.; Waterhouse, A. F.; Whalen, C.; Cuypers, Y.; Bouruet-Aubertot, P.; Ferron, B.; Hibiya, T. A parameterization of local and remote tidal mixing. *Journal of Advances in Modeling Earth Systems* **2020**, *12* (5), e2020MS002065.
(20) Debrot, A. O.; Tiel, A. B.; Bradshaw, J. E. Beach debris in curacao. *Mar. Pollut. Bull.* **1999**, *38* (9), 795−801.
(21) Delandmeter, P.; van Sebille, E. The Parcels v2. 0 lagrangian framework: new field interpolation schemes. *Geoscientific Model Development* **2019**, *12* (8), 3571−3584.
(22) DiBenedetto, M. H.; Ouellette, N. T.; Koseff, J. R. Transport of anisotropic particles under waves. *J. Fluid Mech.* **2018**, *837*, 320−340.
(23) ECMWFIfs documentation cy46r1, part vii: Ecmwf wave model. *IFS Documentation CY46R1*; 2017; DOI: 10.21957/21g1hoiuo.
(24) Egger, M.; Sulu-Gambari, F.; Lebreton, L. First evidence of plastic fallout from the north pacific garbage patch. *Sci. Rep.* **2020**, *10* (1), 7495.
(25) Enders, K.; Lenz, R.; Stedmon, C. A.; Nielsen, T. G. Abundance, size and polymer composition of marine microplastics $\leqslant 10\ \mu$m in the atlantic ocean and their modelled vertical distribution. *Marine pollution bulletin* **2015**, *100* (1), 70−81.
(26) Escudier, R.; Clementi, E.; Nigam, T.; Pistoia, J.; Grandi, A.; Aydogdu, A.*Quality information document (cmems-med-quid-006-004)*; 2021.
(27) Escudier, R.; Clementi, E.; Omar, M.; Cipollone, A.; Pistoia, J.; Aydogdu, A.; Drudi, M.; Grandi, A.; Lyubartsev, V.; Lecci, R.; Cretí, S.; Masina, S.; Coppini, G.; Pinardi, N.*Mediterranean sea physical reanalysis (cmems med-currents, e3r1 system)*; 2020.
(28) Fazey, F. M.; Ryan, P. G. Biofouling on buoyant marine plastics: An experimental study into the effect of size on surface longevity. *Environ. Pollut.* **2016**, *210*, 354−360.
(29) Fischer, R.; Lobelle, D.; Kooi, M.; Koelmans, A.; Onink, V.; Laufkötter, C.; Amaral-Zettler, L.; Yool, A.; van Sebille, E. Modeling submerged biofouled microplastics and their vertical trajectories. *Biogeosciences Discussions* **2021**, *19*, 2211.
(30) Gerritse, J.; Leslie, H. A.; de Tender, C. A.; Devriese, L. I.; Vethaak, A. D. Fragmentation of plastic objects in a laboratory seawater microcosm. *Scientific reports* **2020**, *10* (1), 10945.
(31) Gündoğdu, S.; Çevik, C. Micro-and mesoplastics in northeast levantine coast of turkey: The preliminary results from surface samples. *Mar. Pollut. Bull.* **2017**, *118* (1−2), 341−347.
(32) Hardesty, B. D.; Lawson, T.; van der Velde, T.; Lansdell, M.; Wilcox, C. Estimating quantities and sources of marine debris at a continental scale. *Frontiers in Ecology and the Environment* **2017**, *15* (1), 18−25.
(33) Hersbach, H.; Bell, B.; Berrisford, P.; Hirahara, S.; Horányi, A.; Muñoz-Sabater, J.; Nicolas, J.; Peubey, C.; Radu, R.; Schepers, D.; Simmons, A.; Soci, C.; Abdalla, S.; Abellan, X.; Balsamo, G.; Bechtold, P.; Biavati, G.; Bidlot, e.; Bonavita, M.; De Chiara, G.; Dahlgren, P.; Dee, D.; Diamantakis, M.; Dragani, R.; Flemming, J.; Forbes, R.; Fuentes, M.; Geer, A.; Haimberger, L.; Healy, S.; Hogan, R. J.; Hólm, E.; Janisková, M.; Keeley, S.; Laloyaux, P.; Lopez, P.; Lupu, C.; Radnoti, G.; de Rosnay, P.; Rozum, I.; Vamborg, F.; Villaume, S.; Thépaut, J.-N. The era5 global reanalysis. *Quarterly Journal of the Royal Meteorological Society* **2020**, *146* (730), 1999−2049.
(34) Hinata, H.; Mori, K.; Ohno, K.; Miyao, Y.; Kataoka, T. An estimation of the average residence times and onshore-offshore diffusivities of beached microplastics based on the population decay of tagged meso-and macrolitter. *Marine pollution bulletin* **2017**, *122* (1−2), 17−26.
(35) Houpert, L.; Testor, P.; De Madron, X. D.; Somot, S.; D'ortenzio, F.; Estournel, C.; Lavigne, H. Seasonal cycle of the mixed layer, the seasonal thermocline and the upper-ocean heat storage rate in the mediterranean sea derived from observations. *Progress in Oceanography* **2015**, *132*, 333−352.
(36) Huck, T.; Bajon, R.; Grima, N.; Portela, E.; Molines, J.; Penduff, T. Three-dimensional dispersion of neutral "plastic" particles in a global ocean model. front. *Anal. Sci.* **2022**, *2*, 868515.
(37) Isobe, A.; Iwasaki, S. The fate of missing ocean plastics: Are they just a marine environmental problem? *Sci. Total Environ.* **2022**, *825*, 153935.
(38) Kaandorp, M. L.; Dijkstra, H. A.; van Sebille, E. Closing the mediterranean marine floating plastic mass budget: inverse modeling of sources and sinks. *Environ. Sci. Technol.* **2020**, *54* (19), 11980−11989.
(39) Kaandorp, M. L.; Dijkstra, H. A.; van Sebille, E. Modelling size distributions of marine plastics under the influence of continuous cascading fragmentation. *Environmental Research Letters* **2021**, *16* (5), 054075.
(40) Kaandorp, M. L.; Ypma, S. L.; Boonstra, M.; Dijkstra, H. A.; van Sebille, E. Using machine learning and beach cleanup data to explain litter quantities along the dutch north sea coast. *Ocean Science* **2022**, *18* (1), 269−293.
(41) Kerpen, N. B.; Schlurmann, T.; Schendel, A.; Gundlach, J.; Marquard, D.; Hüpgen, M. Wave-induced distribution of microplastic in the surf zone. *Frontiers in Marine Science* **2020**, *7*, 590565.
(42) Kooi, M.; Nes, E. H. v.; Scheffer, M.; Koelmans, A. A. Ups and downs in the ocean: effects of biofouling on vertical transport of microplastics. *Environ. Sci. Technol.* **2017**, *51* (14), 7963−7971.
(43) Kooi, M.; Reisser, J.; Slat, B.; Ferrari, F. F.; Schmid, M. S.; Cunsolo, S.; Brambini, R.; Noble, K.; Sirks, L.-A.; Linders, T. E.; Schoeneich-Argent, R. I.; Koelmans, A. A. The effect of particle properties on the depth profile of buoyant plastics in the ocean. *Sci. Rep.* **2016**, *6* (1), 33882.
(44) Korres, G.; Ravdas, M.; Zacharioudaki, A.*Mediterranean Sea Waves hindcast (cmems med-waves)*; 2019; DOI: 10.25423/cmcc/medsea_hindcast_wav_006_012.
(45) Kukulka, T.; Proskurowski, G.; Morét-Ferguson, S.; Meyer, D.; Law, K. The effect of wind mixing on the vertical distribution of buoyant plastic debris. *Geophys. Res. Lett.* **2012**, *39* (7), L07601.
(46) Lacerda, A. L. d. F.; Rodrigues, L. d. S.; van Sebille, E.; Rodrigues, F. L.; Ribeiro, L.; Secchi, E. R.; Kessler, F.; Proietti, M. C. Plastics in sea surface waters around the antarctic peninsula. *Sci. Rep.* **2019**, *9* (1), 3977.
(47) Lange, M.; van Sebille, E. Parcels V0.9: Prototyping a lagrangian ocean analysis frameworkfor the petascale age. *Geoscientific Model Development Discussions* **2017**, *10*, 4175−4186.
(48) Large, W. G.; McWilliams, J. C.; Doney, S. C. Oceanic vertical mixing: A review and a model with a nonlocal boundary layer parameterization. *Reviews of geophysics* **1994**, *32* (4), 363−403.

(49) Lebreton, L.; Egger, M.; Slat, B. A global mass budget for positively buoyant macroplastic debris in the ocean. *Sci. Rep.* **2019**, *9* (1), 12922.
(50) Lebreton, L. C.; Van Der Zwet, J.; Damsteeg, J.-W.; Slat, B.; Andrady, A.; Reisser, J. River plastic emissions to the world's oceans. *Nat. Commun.* **2017**, *8*, 15611.
(51) Lebreton, L.-M.; Greer, S.; Borrero, J. C. Numerical modelling of floating debris in the world's oceans. *Marine pollution bulletin* **2012**, *64* (3), 653−661.
(52) Liubartseva, S.; Coppini, G.; Lecci, R.; Clementi, E. Tracking plastics in the mediterranean: 2d lagrangian model. *Marine pollution bulletin* **2018**, *129* (1), 151−162.
(53) Madec, G.; Bourdallé-Badie, R.; Bouttier, P.-A.; Bricaud, C.; Bruciaferri, D.; Calvert, D.; Chanut, J.; Clementi, E.; Coward, A.; Delrosso, D.; Ethé, C.; Flavoni, S.; Graham, T.; Harle, J.; Iovino, D.; Lea, D.; Lévy, C.; Lovato, T.; Martin, N.; Masson, S.; Mocavero, S.; Paul, J.; Rousset, C.; Storkey, D.; Storto, A.; Vancoppenolle, M.*Nemo ocean engine*; 2017; DOI: 10.5281/ZENODO.3248739.
(54) Mascarenhas, R.; Santos, R.; Zeppelini, D. Plastic debris ingestion by sea turtles in Paraíba, brazil. *Marine pollution bulletin* **2004**, *49* (4), 354−355.
(55) McWilliams, J. C.; Sullivan, P. P. Vertical mixing by langmuir circulations. *Spill Science & Technology Bulletin* **2000**, *6* (3−4), 225−237.
(56) Merlino, S.; Locritani, M.; Bernardi, G.; Como, C.; Legnaioli, S.; Palleschi, V.; Abbate, M. Spatial and temporal distribution of chemically characterized microplastics within the protected area of pelagos sanctuary (nw mediterranean sea): Focus on natural and urban beaches. *Water* **2020**, *12* (12), 3389.
(57) Molnar, J. L.; Gamboa, R. L.; Revenga, C.; Spalding, M. D. Assessing the global threat of invasive species to marine biodiversity. *Frontiers in Ecology and the Environment* **2008**, *6* (9), 485−492.
(58) Morales-Caselles, C.; Viejo, J.; Martí, E.; González-Fernández, D.; Pragnell-Raasch, H.; González-Gordillo, J. I.; Montero, E.; Arroyo, G. M.; Hanke, G.; Salvo, V. S.; Basurko, O. C.; Mallos, N.; Lebreton, L.; Echevarría, F.; van Emmerik, T.; Duarte, C. M.; Gálvez, J. A.; van Sebille, E.; Galgani, F.; García, C. M.; Ross, P. S.; Bartual, A.; Ioakeimidis, C.; Markalain, G.; Isobe, A.; Cózar, A. An inshore-offshore sorting system revealed from global classification of ocean litter. *Nature Sustainability* **2021**, *4* (6), 484−493.
(59) Mountford, A.; Morales Maqueda, M. Eulerian modeling of the three-dimensional distribution of seven popular microplastic types in the global ocean. *Journal of Geophysical Research: Oceans* **2019**, *124* (12), 8558−8573.
(60) O'Brine, T.; Thompson, R. C. Degradation of plastic carrier bags in the marine environment. *Marine pollution bulletin* **2010**, *60* (12), 2279−2283.
(61) Onink, V.*Modeling, analysis and visualization code for "The influence of particle size and fragmentation on large-scale microplastic transport in the mediterranean sea" (v1.0)*; 2022.
(62) Onink, V.; Jongedijk, C. E.; Hoffman, M. J.; van Sebille, E.; Laufkötter, C. Global simulations of marine plastic transport show plastic trapping in coastal zones. *Environmental Research Letters* **2021**, *16* (6), 064053.
(63) Onink, V.; van Sebille, E.; Laufkötter, C. Empirical lagrangian parametrization for wind-driven mixing of buoyant particles at the ocean surface. *Geoscientific Model Development* **2022**, *15* (5), 1995−2012.
(64) Onink, V.; Wichmann, D.; Delandmeter, P.; van Sebille, E. The role of ekman currents, geostrophy, and stokes drift in the accumulation of floating microplastic. *Journal of Geophysical Research: Oceans* **2019**, *124* (3), 1474−1490.
(65) Pabortsava, K.; Lampitt, R. S. High concentrations of plastic hidden beneath the surface of the atlantic ocean. *Nat. Commun.* **2020**, *11* (1), 4073.
(66) Pedrotti, M. L.; Mazzocchi, M. G.; Lombard, F.; Galgani, F.; Kerros, M. E.; Henry, M.; Elineau, A.; Petit, S.; Fernandez-de Puelles, M. L.; Gasparini, S.; Tirelli, V.; Jamet, J.-L.; Mossotti, R.TARA mediterranean expedition: assessing the impact of microplastics on mediterranean ecosystem. In *Proceedings of the International Conference on Microplastic Pollution in the Mediterranean Sea*; Springer: 2018; pp 25−29, DOI: 10.1007/978-3-319-71279-6_4.
(67) Pieper, C.; Martins, A.; Zettler, E.; Loureiro, C. M.; Onink, V.; Heikkilä, A.; Epinoux, A.; Edson, E.; Donnarumma, V.; de Vogel, F.; Law, K. L.; Amaral-Zettler, L.Into the med: Searching for microplastics from space to deep-sea. In *International Conference on Microplastic Pollution in the Mediterranean Sea*; Springer: 2019; pp 129−138, DOI: 10.1007/978-3-030-45909-3_21.
(68) Pieper, C.; Ventura, M. A.; Martins, A.; Cunha, R. T. Beach debris in the azores (ne atlantic): Faial island as a first case study. *Marine pollution bulletin* **2015**, *101* (2), 575−582.
(69) Poulain, M.; Mercier, M. J.; Brach, L.; Martignac, M.; Routaboul, C.; Perez, E.; Desjean, M. C.; Ter Halle, A. Small microplastics as a main contributor to plastic mass balance in the north atlantic subtropical gyre. *Environ. Sci. Technol.* **2019**, *53* (3), 1157−1164.
(70) Resmerită, A.-M.; Coroaba, A.; Darie, R.; Doroftei, F.; Spiridon, I.; Simionescu, B. C.; Navard, P. Erosion as a possible mechanism for the decrease of size of plastic pieces floating in oceans. *Marine pollution bulletin* **2018**, *127*, 387−395.
(71) Ruiz-Orejón, L. F.; Sardá, R.; Ramis-Pujol, J. Now, you see me: High concentrations of floating plastic debris in the coastal waters of the balearic islands (spain). *Marine pollution bulletin* **2018**, *133*, 636−646.
(72) Ryan, P. G.; Perold, V.; Osborne, A.; Moloney, C. L. Consistent patterns of debris on south african beaches indicate that industrial pellets and other mesoplastic items mostly derive from local sources. *Environ. Pollut.* **2018**, *238*, 1008−1016.
(73) Semcesen, P. O.; Wells, M. G. Biofilm growth on buoyant microplastics leads to changes in settling rates: Implications for microplastic retention in the great lakes. *Mar. Pollut. Bull.* **2021**, *170*, 112573.
(74) Simon-Sánchez, L.; Grelaud, M.; Garcia-Orellana, J.; Ziveri, P. River deltas as hotspots of microplastic accumulation: The case study of the ebro river (nw mediterranean). *Science of the total environment* **2019**, *687*, 1186−1196.
(75) Song, Y. K.; Hong, S. H.; Jang, M.; Han, G. M.; Jung, S. W.; Shim, W. J. Combined effects of uv exposure duration and mechanical abrasion on microplastic fragmentation by polymer type. *Environ. Sci. Technol.* **2017**, *51* (8), 4368−4376.
(76) Tsiaras, K.; Hatzonikolakis, Y.; Kalaroni, S.; Pollani, A.; Triantafyllou, G. Modeling the pathways and accumulation patterns of micro-and macro-plastics in the mediterranean. *Frontiers in Marine Science* **2021**, *8*, 743117.
(77) Turcotte, D. Fractals and fragmentation. *Journal of Geophysical Research: Solid Earth* **1986**, *91* (B2), 1921−1926.
(78) Van Franeker, J. A.; Law, K. L. Seabirds, gyres and global trends in plastic pollution. *Environmental pollution* **2015**, *203*, 89−96.
(79) van Sebille, E.; Aliani, S.; Law, K. L.; Maximenko, N.; Alsina, J. M.; Bagaev, A.; Bergmann, M.; Chapron, B.; Chubarenko, I.; Cózar, A.; Delandmeter, P.; Egger, M.; Fox-Kemper, B.; Garaba, S. P.; Goddijn-Murphy, L.; Hardesty, B. D.; Hoffman, M. J.; Isobe, A.; Jongedijk, C. E.; Kaandorp, M. L. A.; Khatmullina, L.; Koelmans, A. A.; Kukulka, T.; Laufkötter, C.; Lebreton, L.; Lobelle, D.; Maes, C.; Martinez-Vicente, V.; Maqueda, M. A. M.; Poulain-Zarcos, M.; Rodríguez, E.; Ryan, P. G.; Shanks, A. L.; Shim, W. J.; Suaria, G.; Thiel, M.; van den Bremer, T. S.; Wichmann, D. The physical oceanography of the transport of floating marine debris. *Environmental Research Letters* **2020**, *2* (15), 023003.
(80) van Sebille, E.; Wilcox, C.; Lebreton, L.; Maximenko, N.; Hardesty, B. D.; Van Franeker, J. A.; Eriksen, M.; Siegel, D.; Galgani, F.; Law, K. L. A global lnventory of Small floating plastic debris. *Environmental Research Letters* **2015**, *10* (12), 124006.
(81) Waldschläger, K.; Schüttrumpf, H. Effects of particle properties on the settling and rise velocities of microplastics in freshwater under laboratory conditions. *Environ. Sci. Technol.* **2019**, *53* (4), 1958−1966.
(82) Woodall, L. C.; Sanchez-Vidal, A.; Canals, M.; Paterson, G. L.; Coppock, R.; Sleight, V.; Calafat, A.; Rogers, A. D.; Narayanaswamy,

B. E.; Thompson, R. C. The deep sea is a major sink for microplastic debris. *Royal Society open science* **2014**, *1* (4), 140317.
(83) Wright, S. L.; Thompson, R. C.; Galloway, T. S. The physical impacts of microplastics on marine organisms: a review. *Environmental pollution* **2013**, *178*, 483−492.
(84) Zeri, C.; Adamopoulou, A.; Koutsikos, N.; Lytras, E.; Dimitriou, E. Rivers and wastewater-treatment plants as microplastic pathways to eastern mediterranean waters: First records for the aegean sea, greece. *Sustainability* **2021**, *13* (10), 5328.
(85) Zhao, D.; Li, M. Dependence of wind stress across an air-sea interface on wave states. *Journal of Oceanography* **2019**, *75* (3), 207−223.
(86) Zhao, S.; Zettler, E. R.; Bos, R. P.; Lin, P.; Amaral-Zettler, L. A.; Mincer, T. J. Large quantities of small microplastics permeate the surface ocean to abyssal depths in the south atlantic gyre. *Global Change Biology* **2022**, *9* (28), 2991−3006.
(87) Zhu, L.; Zhao, S.; Bittar, T. B.; Stubbins, A.; Li, D. Photochemical dissolution of buoyant microplastics to dissolved organic carbon: rates and microbial impacts. *Journal of hazardous materials* **2020**, *383*, 121065.

https://doi.org/10.1021/acs.est.2c03363
Environ. Sci. Technol. 2022, 56, 15528−15540